Conformational Disorder of Proteins Assessed by Real-Space Molecular Dynamics Refinement

Zhi Chen* and Michael S. Chapman†
Departments of *Physics and †Chemistry and Institute of Molecular Biophysics, Florida State University, Tallahassee, Florida 32306 USA

ABSTRACT Motion is critical to the function of many proteins, but much more difficult to study than structure. Due to lack of easy alternatives, although there are inherent limitations, there have been several prior attempts to extract some information from the Bragg scattering in conventional diffraction patterns. Bragg diffraction reflects only a small proportion of a protein's motion and disorder, so fitted values likely underestimate reality. However, this work shows that the fitted estimates should be even smaller, because current methods of refinement over-fit the Bragg diffraction, leading to a component of the disorder that is not based on any experimental data, and could be characterized as a guess. Real-space refinement is less susceptible than other methods, but its application depends on the availability of very accurate experimental phases. A future challenge will be the collection of such data without resort to cryo-techniques, so that a physiologically relevant understanding can be achieved.

INTRODUCTION

Spectroscopic experiments and molecular dynamics (MD) simulations indicate that protein molecules sample a large number of distinct conformations (Ansari et al., 1987; Brooks et al., 1988). Crystallographic analyses confirm this, but the usual analysis of Bragg diffraction cannot distinguish temporal from spatial disorder, i.e., conformations that change over time or that differ between molecules in the crystalline lattice. Conventional macromolecular crystallographic analysis is further limited in that, with few exceptions (see below), coupling of motions is ignored, only the harmonic component of disorder/motion is modeled, and anisotropic motions can often be represented only by isotropic approximations at the resolution experimentally attainable.

Atomic motion is likely at the heart of many biochemical processes: catalysis, control, communication, and motility. It has proved more difficult to characterize the motion than the average structure. Although conventional crystallographic techniques are inherently ill suited, difficulties in other techniques have encouraged efforts to glean as much as possible from Bragg diffraction data. It has long been standard procedure to refine against the data the values of thermal parameters or *B*-factors (Debye, 1912) that can account for harmonic motions of an atom about its centroid. However, there is ample evidence that such modeling of harmonic components significantly underestimates the total disorder in protein crystals (Thune and Badger, 1995).

Received for publication 29 December 1999 and in final form 19 December 2000.

Z. Chen's current address: Computer Science Department, CB 3175, University of North Carolina, Chapel Hill, NC 27599.

Address reprint requests to Dr. Michael S. Chapman, Institute of Molecular Biophysics, Florida State University, Tallahassee, FL 32306-4380. Tel.: 850-644-8354; Fax: 850-561-1406; E-mail: chapman@sb.fsu.edu.

0006-3495/01/03/1466/07 $2.00

This work follows a series of efforts that have sought to model the anharmonic components by replacing a single molecular model with an ensemble. After fitting to the diffraction data, the ensemble is supposed to representatively sample the available conformations (Burling and Brünger, 1994; Burling et al., 1996; Clarage and Phillips, 1994; Gros et al., 1990; Kuriyan et al., 1991; Pellegrini et al., 1997). Several of these related approaches were successful to the extent that the resulting ensemble of models had improved agreement to the diffraction data (relative to a single model).

Ensembles have many more degrees of freedom than the corresponding single model, so a central question is how much of the improved fit is due to absolute model improvement versus meaningless over-fitting. The entry of cross-validation and free *R*-factors into these analyses was a landmark (Brünger, 1992). Assessment of the fit of models to a subset of the data excluded from refinement provided an independent appraisal of quality.

Free *R*-factors have confirmed that ensembles can be an improvement upon a single conformer model. However, it is a concern that most of the prior ensemble refinements showed symptoms of over-fitting (Brünger, 1997): 1) conventional (self-validated) *R*-factors that decreased more with ensemble size than the cross-validated R^{free} and 2) the absence of a sharp minimum of R^{free} versus ensemble size. These symptoms occur even with highly constrained refinements (Pellegrini et al., 1997). It will be shown here that some over-fitting is unavoidable with many of the prior methods. We search for improved methods and consider the systematic errors of over-fitting in a multi-conformer refinement.

Over-fitting can be particularly pernicious in multi-conformer refinement, because it increases the estimate of the number of conformers in the ensemble. This leads to a systematic overestimation of components of the disorder that are probed by Bragg diffraction. The overestimate may still be less than the real disorder, but this is because Bragg

diffraction measures only part of the disorder. Even if only a small part of the total real disorder, our models should account only for the measurable disorder. Anything beyond this is guesswork.

Although cross-validated free *R*-factors are the best indicator of over-fitting, they are not perfect in this application. Multi-conformer refinement is similar to a method for single-conformer refinement advocated by Brünger (1997). MD refinement is repeated with different starting random seeds, so that the best can be selected. Starting point, refinement path, and chance affect slightly the final model configuration. In any one model, some regions will be better than others, but as an ensemble increases in size, there is an increasing chance that the best possible local configuration is found in at least one of the family. As demonstrated with simulated data, the average model is improved in ensemble refinement relative to a single model (Pellegrini et al., 1997). An R^{free} that decreases with increasing ensemble size could indicate either or both of the following: that additional disorder is warranted or that the average structure is better refined with an ensemble of starting points. It is conceivable that over-fitting of disorder could increase even as R^{free} decreases, if there is an offsetting improvement of the average structure. Thus, other signs of over-fitting will be explored.

Earlier work with single-conformer refinement had demonstrated that real-space refinement was less subject to over-fitting than conventional reciprocal-space methods (Chapman and Blanc, 1997; Zhou et al., 1999). Here, applied to ensembles, R^{free} indicates that maximum-likelihood reciprocal-space methods give a slightly better average structure than real-space methods. However, evidence will be presented that real-space-refined ensembles are less over-fit and give a more realistic assessment of the Bragg component of disorder.

Why should real-space methods be expected to reduce over-fitting? One source of improvement is the implicit use of experimental phases, improving the data:parameter ratio. Comparisons with phase-restrained or structure factor vector refinements conducted in reciprocal space show that this is not the only source of improvement (Zhou et al., 1999). In any reciprocal-space refinement, the fittings of different parts of the model are interdependent, because each calculated structure factor has a contribution from every atom. Over-fitting has been characterized in which one region adjusts away from its correct structure to compensate for deficiencies of another part of the model and to restore good overall agreement of structure factors (Hodel et al., 1992). Deficiencies include not only model errors, but also inadequate modeling of disordered solvent or protein, and remain in many macromolecular structures refined to $R \approx 0.2$. In a true real-space refinement, remote interdependencies can be eliminated, because the fit to the local electron density is independent of distant regions. Therefore there is much less propensity for over-fitting.

There are two caveats to real-space refinement. First, once calculated phases are used, real- and reciprocal-space refinements become more equally prone to over-fitting, because remote regions become interlinked through the phasing (Chapman and Blanc, 1997). Second, phases are rarely as accurate as measured amplitudes, so their use in real-space refinement can limit the final fit to amplitudes (so R and R^{free} are often higher) (Chen et al., 1999b). Thus, the real-space approach would be most applicable to an example for which there were available very accurate experimental phases. The 1.8-Å structure of mannose-binding protein A (MBP) was determined using phases from the strong anomalous scattering of a bound lanthanide collected with synchrotron radiation at three wavelengths (Burling et al., 1996). The phases have been determined with unusual accuracy, making MBP a good candidate for studies such as these (Burling et al., 1996; Chen et al., 1999b).

Application of the real-space methods to MBP yielded disorder of smaller magnitude than previously reported for other systems and methods. Our example application is analyzed with respect to the types of motion and disorder that might occur in proteins. In the current work, the chief limitation is that the data most amenable to analysis come from experiments performed at cryo-temperatures. This limitation will likely soon be overcome, but the current analysis of a protein at ~110 K may represent only part of the disorder at physiological temperatures (~310 K).

MATERIALS AND METHODS

Refinement tests compared three target functions: 1) real space (Chapman, 1995):

$$E_{\text{xray}}(\rho) = \int (\rho_{\text{c}} - \rho_{\text{o}})^2 dv,$$

2) conventional reciprocal space residual (Hendrickson, 1985):

$$E_{\text{xray}}(F) = \sum_{\vec{h}} (|\vec{F}_{\text{c}}(\vec{h})| - |\vec{F}_{\text{o}}(\vec{h})|)^2,$$

and 3) maximum likelihood (Adams et al., 1997; Pannu and Read, 1996):

$$E^{\text{ML}}_{\text{xray}}\{P(|\vec{F}_{\text{o}}|; |\vec{F}_{\text{c}}|)\} = -\sum_{\vec{h}} \log\{P(|\vec{F}_{\text{o}}(\vec{h})|; |\vec{F}_{\text{c}}(\vec{h})|)\}$$

$$\approx \sum_{\vec{h}} \frac{1}{\sigma^2_{\text{ML}}} (|\vec{F}_{\text{o}}(\vec{h})| - \langle|\vec{F}_{\text{o}}(\vec{h})|\rangle)^2,$$

using an implementation that optimizes the agreement with the ABCD Hendrickson-Lattmann coefficients of the phase probability distribution (Pannu et al., 1998).

In the formulae above, ρ is the electron density; subscripts o and c indicate (experimentally) observed and calculated (from model), respectively, v is the molecular volume, $F(h)$ is the structure factor for reflection h, and scaling is implicitly assumed.

These types of refinement are in widespread use, except perhaps for real-space refinement. Real-space refinement differs in that the optimiza-

tion is of the fit of the model to electron density (instead of diffraction amplitudes). The method differs from earlier real-space methods in that it accounts rigorously for the experimental resolution and is fully restrained to standard stereochemistry in ways identical to modern reciprocal-space methods. For this work, an implementation was used in which the real-space residual is defined as an alternate target for the XPlor program (Brünger et al., 1987; Chen et al., 1999b). The programs X-plor (Brünger et al., 1987) and CNS (Brünger et al., 1998) were used for reciprocal-space refinements, so that for all trials, compatible annealing protocols, weights, and optimization strategies could be used.

First, the methods were tested with simulated diffraction data. Data were calculated from the structure of α-amylase inhibitor (Pflugrath et al., 1989) after applying MD without any restraints to x-ray crystallographic data. The annealing protocol started at 2500 K and dropped to 300 K. Three individual simulations using different random seeds were used to generate a three-fold ensemble with R/R^{free} of 0.475/0.478 for simulated data between 2.0 and 17 Å resolution. As with applications to real data, tests with simulated data were evaluated using cross-validated free R-factors (Brünger, 1997). In addition, for the simulations, it was possible to calculate positional deviations of refined models from those used to calculate the simulated data.

In applications to real data, coordinates and B-factors from the published 1.8-Å MBP structure (Protein Data Bank entry 1YTT; Burling et al., 1996) were used for the starting model, with copies made to generate multiple conformations. Occupancy of each conformer was taken as the inverse of the number of conformers and fixed throughout the refinement. The database coordinates contained alternate structures for a few amino acids, but these alternates were ignored for this work. Refinement was run in a mode in which stereochemical interactions were considered within a conformer but ignored between different conformers (Burling et al., 1997). Appropriate weighting between stereochemical and diffraction terms was evaluated for each ensemble size by repeating the entire refinement with several weights until that with lowest R^{free} was found (Brünger, 1992).

Cross-validated free R-factors were calculated with a random 4% subset that was removed from the data set before refinement and to map calculation (Brünger, 1997). To mitigate the effect of data omission on the real-space refinement, a published modification to the cross-validation procedure was used in which the 4%-test set was replaced (rather than omitted) by the resolution-shell average amplitude, a nonbiased substitute (Chen et al., 1999a). This substituted data set was used to calculate the map for real-space refinement. The map used for real-space refinement was calculated using phases derived from the published multi-wavelength anomalous diffraction (Burling et al., 1996).

The same refinement protocol was used for each method of refinement. Torsion-angle MD was used (Rice and Brünger, 1994) to limit the number of free parameters. Starting at a simulated temperature of 2500 K, the system was annealed to 300 K in ~2.4 ps. This was followed by a short period of relaxation through MD in Cartesian space. Then the system was optimized through conjugate gradient minimization, with B-factors refined in the final cycles. Solvent molecules and lanthanide ions were fixed during MD but released in the final energy minimization.

Coordinate sets resulting from the refinements were analyzed in a variety of ways that will be detailed in the Results. These included calculations of the deviations between ensemble members at each amino acid, and overall. These were first analyzed with respect to the method of refinement and then to determine the sites of greatest conformational variability within MBP. The following method was used to detect potential hinge motions. In gross approximation, it was reasoned that the displacement of atoms about a hinge point should be proportional to the angle of rotation multiplied by distance from the hinge. Distance from the hinge was crudely approximated by distance along the covalent backbone. In turn, every backbone torsion angle was tested as a potential hinge point. Correlation coefficients were calculated between actual Cartesian atomic deviations (within the ensemble) and those calculated from distance times the deviation in hinge torsion angle for segments of one to nine residues. The segment length with highest correlation was taken as the size of fragment that might possibly be undergoing a hinge motion. Maximal correlation coefficients less than 0.5 were interpreted as the absence of a hinge motion.

RESULTS

In tests against data simulated from an ensemble of three α-amylase models, all methods of refinement generate ensembles whose average structures approximate the target ensemble (Table 1). In order of decreasing quality, they rank real-space, maximum-likelihood, and reciprocal-space. In terms of the fitted disorder (Table 2), with the reduced over-fitting of simulated data (see below), all refinement methods underestimate the disorder of the target, but once again, they rank in the same order: real-space coming slightly closer than maximum-likelihood, with both being substantially better than conventional reciprocal-space methods.

The data in tables 1 and 2 were calculated with the benefit of knowing what the solution should be. What would we be able to tell with only cross-validated R-factors to guide us? In refinements against the simulated data, all methods correctly determine the number of conformers (Fig. 1). Differences between the methods are marginal in these contrived simulations.

Although the simulations are a necessary test that the programs run as intended, they are very unrealistic and poor predictors of performance with real data. First, real-space and phase-restrained methods have the unrealistic advantage of perfect phases. Second, the potential for over-fitting is very much smaller with simulated data; there is neither experimental error nor disordered protein/solvent. Thus, the model can be a fuller description of the simulated diffraction data. Our experience with real data, with which over-fitting is an important concern, is somewhat different.

With real MBP diffraction data, ensembles were an improvement over a single-conformer model, regardless of the method of refinement (Fig. 2). Evidence of over-fitting, particularly the statistic $\Delta R = R^{free} - R$ (Brünger, 1997), depended on the method of refinement. As with single-conformer refinement (Chapman and Blanc, 1997; Zhou et al., 1999), conventional reciprocal-space methods proved to be the most susceptible to over-fitting upon the addition of conformers. The drop in R is 2.5 times that of R^{free}, sug-

TABLE 1 Tests of refinement using simulated diffraction data calculated from an ensemble of three model structures

	Refinement method		
	Least-squares reciprocal-space	Maximum-likelihood, phase-restrained	Real-space
Backbone	0.056 Å	0.050 Å	0.049 Å
All non-H atoms	0.208 Å	0.143 Å	0.135 Å

Data are RMSDs comparing the centroid atom positions of 3-mer refined ensembles against those of the ensemble from which the data were simulated.

TABLE 2 Tests of refinement using simulated diffraction data calculated from an ensemble of 3 model structures

Number of conformers	Refinement method			
	None: ensemble from which $\|F\|$s calculated	Least-squares reciprocal-space	Maximum-likelihood, phase-restrained	Real-space
2		0.343 Å	0.487 Å	0.516 Å
3	0.749 Å	0.393 Å	0.598 Å	0.621 Å
4		0.524 Å	0.703 Å	0.697 Å
5		0.509 Å	0.723 Å	0.711 Å
6		0.598 Å	0.759 Å	0.744 Å

RMSD between individual members of ensembles refined by several methods against the 3-mer simulated data.

gesting that much of the modeled disorder has little basis in reality.

The real-space approach as well as the phase-restrained maximum-likelihood (ML) method (which became available during our work) show little or no evidence of over-fitting in ΔR. In fact, the negative value of ΔR suggests that the addition of conformers allowed ML refinement to find an improved average structure (Pellegrini et al., 1997), undoing some prior over-fitting. It is phase-restrained ML methods that give the best average structure.

The differences in R^{free} between real-space and ML refined models are similar in single-conformer (Chen et al., 1999b) and multi-conformer refinements (a difference of 0.010 Å for a single conformer cf. a difference of 0.012 Å for multiconformer), suggesting similar causes for performance differences. Slightly poorer real-space performance for single conformers (Chen et al., 1999b) was due to phase error in even this unusually accurate phase set (Burling et al., 1996). ML methods can use a weighted multimodal phase probability distribution, but in map calculation for real-space refinement, phases can be weighted, but their distributions are effectively reduced to a unimodal approximation.

The drawback to ML methods is the lack of indication of the magnitude of the disorder. Unlike the other methods, there is no optimum in R^{free} at approximately three conformers (Fig. 2). With the addition of a fourth conformer, R^{free} gives no indication of the over-fitting that is taking place. If there were no over-fitting, addition of conformers beyond the optimal should more appropriately sample the

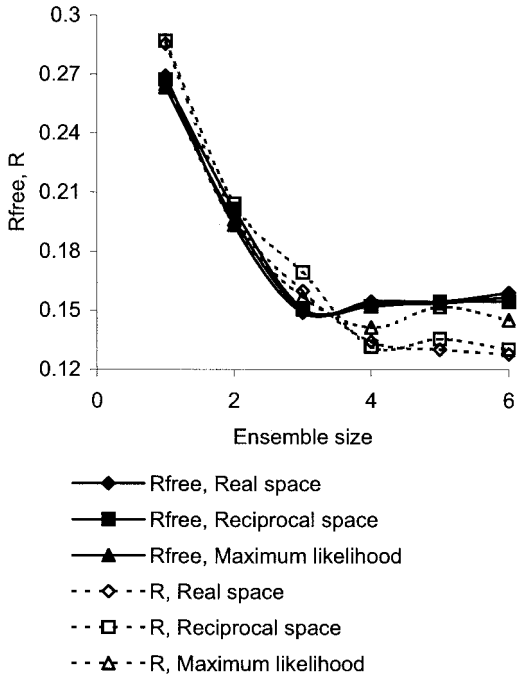

FIGURE 1 Tests against simulated data. An ensemble of three structures was generated by applying molecular dynamics without any experimental (diffraction) restraint. Diffraction data were calculated for the ensemble and used for the refinement of a new set of ensembles of various sizes. Several methods of refinement were used. The minima in R^{free} demonstrate that all of these methods can determine the correct size of the ensemble with error-free data and complete models.

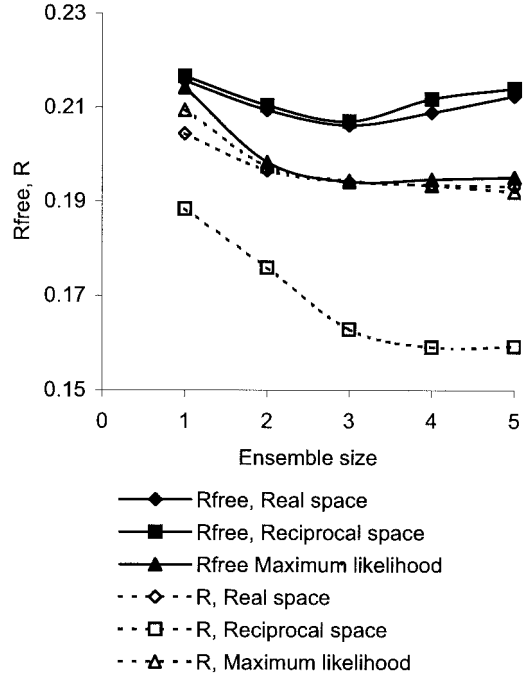

FIGURE 2 *R*-factors as a function of ensemble size for various refinement targets, using the actual MBP diffraction data.

distribution of conformers, but should not systematically increase the variance. The monotonic increase in root mean square deviation (RMSD) between structures (Fig. 3) is evidence of the propensity of even ML methods to over-fit in ensemble refinement.

It is striking that plots of RMSD versus ensemble size are biphasic for all refinement methods (Fig. 3). Deviations increase at a high rate until the ensemble contains the optimal number of conformers. Then RMSDs increase approximately linearly at rates that depend mostly on the refinement method. The increased deviation in the second phase does little to improve the fit to diffraction data. If not over-fitting, this increase is at least gratuitous. It is likely that this over-fitting does not start suddenly with the change of gradient in Fig. 3, but is a component of the fitted disorder, even for small ensemble number. Thus, the overall fitted disorder is a sum of components: 1) real disorder reflected in Bragg diffraction and 2) mere over-fitting. The first component diminishes to zero beyond the optimum, allowing the magnitude of the over-fitting to be estimated by extrapolating the second slope back to a single conformer. As previously indicated, the over-fitting is dependent upon refinement method, but as expected, the extrapolations approximately intersect at a single conformer. This gives us some confidence in subtracting an over-fitting component. A plot of such a corrected RMSD versus ensemble size (Fig. 4) is now asymptotic at the optimal ensemble size (as expected prima facie), and all methods give the same magnitude of disorder: RMSD = 0.29 ± 0.1 Å.

All of the tested refinement methods overestimate the Bragg component of disorder. Real-space methods over-fit least, as evident from the closer agreement of corrected (0.29 Å) and uncorrected RMSDs at the optimum (0.33 Å compared with 0.37 and 0.39 Å for reciprocal-space methods). The real-space refined ensemble structures were analyzed for what they might tell us about the types of disorder present in a protein structure at 110 K. There were few surprises.

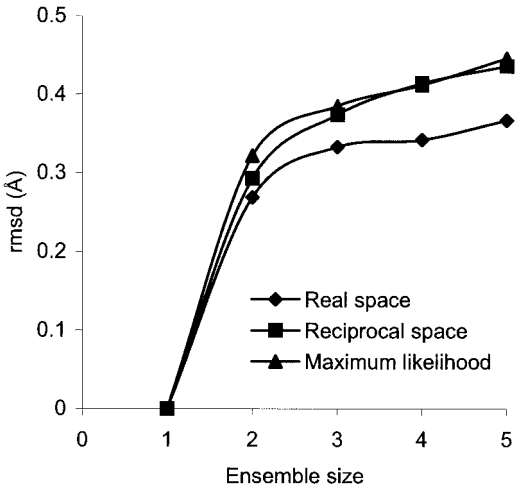

FIGURE 3 RMSD (Å) between MBP conformers as a function of ensemble size.

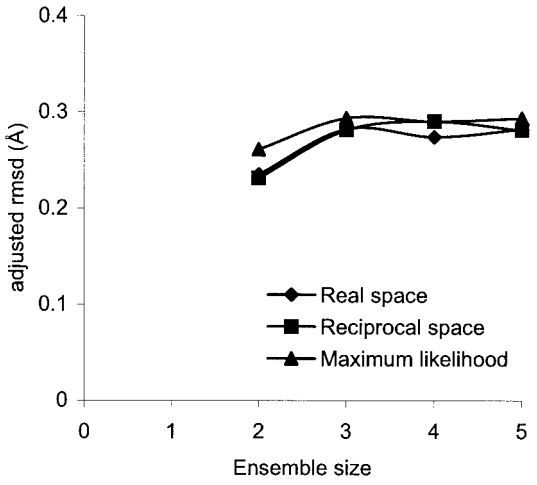

FIGURE 4 Adjusted RMSD between MBP conformers as a function of ensemble size, where the linear increase of RMSD with ensemble size has been subtracted. It is argued in the text that this more faithfully represents the magnitude of the disorder visible in the experimental Bragg diffraction data.

RMSDs of backbone atoms correlate well with the *B*-factors refined for a single conformer ($r = 0.80$). The estimated overall RMSD = 0.29 Å would contribute a very modest 7.4 Å^2 to the *B*-factors, in contrast to some prior results (e.g., Pellegrini et al., 1997) where *B*-factor refinement of a single structure represented only a small fraction of the deviation in a multi-copy ensemble. This difference could be the result of different data analysis or the different sample temperatures. RMSDs also correlate well with surface accessibility ($r = 0.68$), showing the expected dependence of disorder on location within the structure.

Conformational differences between members of the ensemble are primarily local. The correlation distance of backbone torsion angle changes is short (Fig. 5), implying that

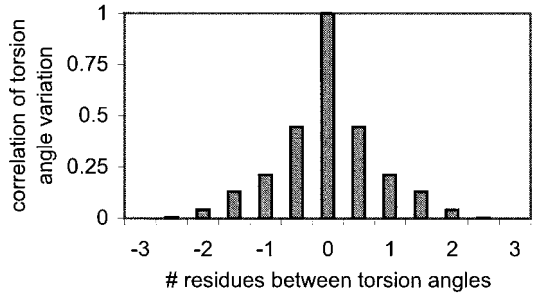

FIGURE 5 Correlation of the magnitude of MBP backbone torsion angle deviation (between conformers) with those of immediate neighbors on the N-terminal (negative) and C-terminal (positive) sides. The observation that the correlation does not extend far indicates that most changes are local to a single amino acid or to segments of at most three amino acids.

most changes are local to a single amino acid, or at most to a segment of three. There are no large or long-range hinge motions. In fact, such correlations extended over at most two amino acids (Fig. 6). Inspection of the ensemble with molecular graphics (Jones et al., 1991) confirmed the absence of long-range changes.

Deviations between ensemble members were also analyzed as a function of residue type. There were no surprises. Backbone differences were largest for glycines. Long side chains (Arg, Glu, and Lys) had larger than average differences (Table 3). There were few examples of side chains showing alternate conformers, perhaps because of the cryo-temperatures used in collecting the data (Burling et al., 1996). Multiple rotamers were detected automatically at Glu A185, Cys A195, Cys A209, Cys A217, Glu B117 and Arg B132, and Cys B217, totaling 7 of 227 residues. Electron density supporting the multiple rotamers was apparent (retrospectively), although it was weak at four of the sites: Glu A185, Cys A209, Glu B117, and Arg B132.

Molecular graphics (Jones et al., 1991) was used to inspect the regions of greatest change. In a small number of cases, the changes were questionable. The side chains of Arg 132, Glu 185, and Cys 209 found alternative rotamers for which the density was weak and could have been noise. However, the electron density justified most of the alternative conformations. For example, refinement successfully found (automatically) the alternate conformations of the Cys 128-Cys 217 disulfide interaction that had been built manually in the published structure (Burling et al., 1996).

TABLE 3 RMSD of corresponding atomic positions between ensemble members as a function of residue type

		RMSD (Å)	
Amino acid	Number	Backbone	All atoms
GLY	18	0.469	0.506
LYS	16	0.421	0.668
SER	15	0.401	0.484
ALA	17	0.397	0.431
CYS	08	0.375	0.497
ARG	08	0.371	0.592
ASP	12	0.371	0.513
GLN	06	0.364	0.577
LEU	10	0.357	0.447
GLU	20	0.352	0.596
THR	18	0.351	0.447
VAL	18	0.350	0.416
ILE	10	0.326	0.407
TYR	04	0.312	0.377
PRO	07	0.305	0.396
ASN	14	0.288	0.394
PHE	12	0.286	0.350
MET	04	0.282	0.379
TRP	04	0.273	0.352
HIS	06	0.215	0.426

These data result from the real-space refinement.

DISCUSSION

This study gives an impression of disorder in a crystalline protein that is much less than previously reported. This is partly because the methods introduced here more narrowly limit the ensemble to the disorder component of the measurable Bragg diffraction. It may also be that many motions of a protein at physiological temperatures are frozen out at temperatures of ~110 K. These are important issues due to the potential impact of motion on function. With increasing numbers of structures determined at cryo-temperatures it will be important to characterize differences from their counterparts at physiological temperatures. Further study should be a priority.

Our results suggest where emphasis should be placed in these future studies. All current methods of refinement over-model the component of the disorder that are visible in Bragg diffraction. ML methods are a substantial improvement on conventional refinement. They give the best-fitting structure. However, as with other reciprocal-space methods, it appears that the amount of disorder fitted is larger than indicated by the Bragg diffraction. Real-space analysis is less susceptible to this over-modeling and the best way to estimate the Bragg component of disorder. However, to rival a ML refinement, the experimental phases must be of the highest quality. Perhaps of greatest impact in analyzing motion/disorder would be precise amplitudes and phases determined experimentally from samples at physiological temperatures. It will be a real challenge to rival the precision of the experimental phases used here (Burling et al., 1996) without the benefits of cryo-cooled samples, but success will be key to further our understanding of motion and disorder.

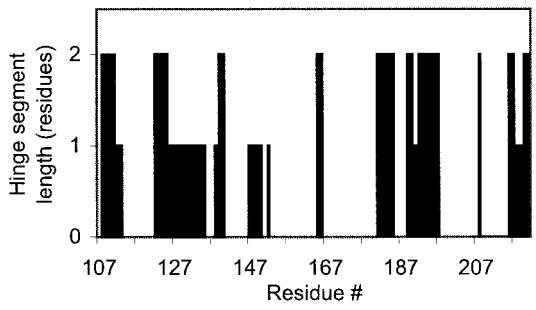

FIGURE 6 Potential hinge motions. As a function of residue number, the vertical axis shows the number of amino acids over which a change in backbone torsion angle is best correlated with the changes in (Cartesian) atomic positions. The maximal correlation distance of two amino acids shows that there are no long-range hinge motions.

We are grateful to Temple Burling and Axel Brünger for access to the MBP coordinates and diffraction data.

This work was supported by the National Science Foundation (BIR94–18741 and DBI98–08098).

REFERENCES

Adams, P. D., N. S. Pannu, R. J. Read, and A. T. Brünger. 1997. Cross-validated maximum-likelihood enhances simulated annealing crystallographic refinement. *Proc. Natl. Acad. Sci. U.S.A.* 94:5018–5023.

Ansari, A., J. Berendzen, D. Braunstein, B. R. Cowen, H. Frauenfelder, M. K. Hong, I. E. Iben, J. B. Johnson, P. Ormos, T. B. Sauke, R. Scholl, A. Schulte, P. J. Steinbach, J. Vittitow, and R. D. Young. 1987. Rebinding and relaxation in the myoglobin pocket. *Biophys. Chem.* 26: 337–355.

Brooks, C. L., M. Karplus, and B. M. Pettitt. 1988. Proteins: a theoretical perspective of dynamics, structure and thermodynamics. *Adv. Chem. Phys.* 71:7–21.

Brünger, A. T. 1992. Free R value: a novel statistical quantity for assessing the accuracy of crystal structures. *Nature.* 355:472–475.

Brünger, A. T. 1997. The free *R* value: a more objective statistic for crystallography. *Methods Enzymol.* 277:366–396.

Brünger, A. T., P. D. Adams, G. M. Clore, P. Gros, R. W. Gross-Kunstleve, J.-S. Jiang, J. Kurzewski, M. Nilges, N. S. Pannu, R. J. Read, L. M. Rice, T. Simonson, and G. L. Warren. 1998. Crystallogaphy and NMR system: a new software system for macromolecular structure determination. *Acta Crystallogr.* D54:905–921.

Brünger, A. T., J. Kuriyan, and M. Karplus. 1987. Crystallographic R factor refinement by molecular dynamics. *Science.* 235:458–460.

Burling, T., P. Adams, and A. T. Brünger. 1997. Multiconformer refinement using very accurate experimental crystallographic phases. *In* Direct Methods for Solving Macromolecular Structures. Lecture notes. S. Fortier, editor. Kluwer, Dordrecht, The Netherlands. 471–477.

Burling, F. T., and A. T. Brünger. 1994. Thermal motion and conformational disorder in protein crystal structures: comparison of multiconformer and time-averaging models. *Israel J. Chem.* 34:165–174.

Burling, F. T., W. I. Weis, K. M. Flaherty, and A. Brünger. 1996. Direct observation of protein solvation and discrete disorder using experimental crystallographic phases. *Science.* 271:72–77.

Chapman, M. S. 1995. Restrained real-space macromolecular atomic refinement using a new resolution-dependent electron density function. *Acta Crystallogr.* A51:69–80.

Chapman, M. S., and E. Blanc. 1997. Potential use of real space refinement in protein structure determination. *Acta Crystallogr.* D53:203–206.

Chen, Z., E. Blanc, and M. S. Chapman. 1999a. Improved free R-factors for the cross-validation of structures. *Acta Crystallogr.* D55:219–224.

Chen, Z., E. Blanc, and M. S. Chapman. 1999b. Real space molecular dynamics refinement. *Acta Crystallogr.* D55:464–468.

Clarage, J. B., and G. N. Phillips. 1994. Cross-validation tests of time-averaged molecular dynamics refinements for determination of protein structures by protein crystallography. *Acta Crystallogr.* D50:24–36.

Debye, P. 1912. Interferenz von Röntgenstrahlen und Wärmebewegung. *Ann. Phys.* 43:49–95.

Gros, P., W. F. van Gunsteren, and W. G. J. Hol. 1990. Inclusion of thermal motion in crystallographic structures by restrained molecular dynamics. *Science.* 249:1149–1152.

Hendrickson, W. W. 1985. Stereochemically restrained refinement of macromolecular structures. *Methods Enzymol.* 115:252–270.

Hodel, A., S.-H. Kim, and A. T. Brünger. 1992. Model bias in macromolecular crystallography. *Acta Crystallogr.* A48:851–858.

Jones, T. A., J.-Y. Zou, S. W. Cowan, and M. Kjeldgaard. 1991. Improved methods for building protein models in electron density maps and the location of errors in these models. *Acta Crystallogr.* A47:110–119.

Kuriyan, J., K. Osapay, S. K. Burley, A. T. Brünger, and W. A. Hendrickson. 1991. Exploration of disorder in protein structures by x-ray restrained molecular dynamics. *Proteins.* 10:340–358.

Pannu, N. S., G. N. Murshudov, E. J. Dodson, and R. J. Read. 1998. Incorporation of prior phase information strengthens maximum-likelihood structure refinement. *Acta Crystallogr.* D54:1285–1294.

Pannu, N. S., and R. J. Read. 1996. Improved structure refinement through maximum likelihood. *Acta Crystallogr.* A52:659–668.

Pellegrini, M., N. Gronbech-Jensen, J. A. Kelly, G. M. Pfluegl, and T. O. Yeates. 1997. Highly constrained multiple-copy refinement of protein crystal structures. *Proteins.* 29:426–432.

Pflugrath, J. W., G. Wiegand, R. Huber, and L. Vertesey. 1989. Crystal structure determination, refinement, and the molecular model of the α-amylase inhibitor Hoe-467A. *J. Mol. Biol.* 189:383–386.

Rice, L. M., and A. T. Brünger. 1994. Torsion angle dynamics: reduced variable conformational sampling enhances crystallographic structure refinement. *Proteins.* 19:277–290.

Thune, T., and J. Badger. 1995. Thermal diffuse x-ray scattering and its contribution to understanding protein dynamics. *Prog. Biophys. Mol. Biol.* 63:251–276.

Zhou, G., T. Somasundaram, E. Blanc, Z. Chen, and M. S. Chapman. 1999. Critical initial real-space refinement in the structure determination of arginine kinase. *Acta Crystallogr. D Biol. Crystallogr.* 55:835–845.